



Dispersion-Flattened Composite Highly Nonlinear Fibre Optimised for Broadband Pulsed Four-Wave Mixing

Lillieholm, Mads; Galili, Michael; Oxenløwe, Leif Katsuo

Published in:

Proceedings of European Conference on Optical Communications 2016

Publication date:

2016

Document Version

Peer reviewed version

[Link back to DTU Orbit](#)

Citation (APA):

Lillieholm, M., Galili, M., & Oxenløwe, L. K. (2016). Dispersion-Flattened Composite Highly Nonlinear Fibre Optimised for Broadband Pulsed Four-Wave Mixing. In Proceedings of European Conference on Optical Communications 2016 (pp. 330-332). VDE Verlag.

General rights

Copyright and moral rights for the publications made accessible in the public portal are retained by the authors and/or other copyright owners and it is a condition of accessing publications that users recognise and abide by the legal requirements associated with these rights.

- Users may download and print one copy of any publication from the public portal for the purpose of private study or research.
- You may not further distribute the material or use it for any profit-making activity or commercial gain
- You may freely distribute the URL identifying the publication in the public portal

If you believe that this document breaches copyright please contact us providing details, and we will remove access to the work immediately and investigate your claim.

Dispersion-Flattened Composite Highly Nonlinear Fibre Optimised for Broadband Pulsed Four-Wave Mixing

Mads Lillieholm⁽¹⁾, Michael Galili⁽¹⁾ and Leif K. Oxenløwe⁽¹⁾

⁽¹⁾ DTU Fotonik, Technical Univ. of Denmark, Bldg. 343, DK-2800, Denmark, madsl@fotonik.dtu.dk

Abstract We present a segmented composite HNLF optimised for mitigation of dispersion-fluctuation impairments for broadband pulsed four-wave mixing. The HNLF-segmentation allows for pulsed FWM-processing of a 13-nm wide input WDM-signal with -4.6-dB conversion efficiency.

Introduction

Four-wave mixing (FWM) using pulsed or continuous wave (CW) pumps have very different requirements on the dispersive properties of the nonlinear material used¹. In our recent study¹, we show how the FWM bandwidth for a pulsed pump is strongly dependent on the third order dispersion (β_3), whereas CW FWM is more dependent on β_2 and β_4 . Therefore, CW FWM, as e.g. widely used for optical phase conjugation²⁻³, will often require a different nonlinear material than e.g. (chirped) pulsed FWM, as often used in e.g. time lens applications⁴⁻⁶.

The highly nonlinear fibre (HNLF) is one of the most common media for nonlinear signal processing, although the control of the zero-dispersion wavelength (ZDW) over the fibre length is a major challenge. However, for long fibre lengths a very high FWM conversion efficiency may be obtained. The SPINE-HNLF⁷ is a type of nonlinear fibre designed to keep the ZDW very stable, though with a relatively large dispersion slope limiting the pulsed FWM bandwidth.

In this paper we present a composite dispersion-flattened HNLF (DF-HNLF), consisting of ~50-m segments arranged to mitigate ZDW fluctuations which impair the FWM bandwidth. The fibre segments are arranged in a ZDW “rapid-map”, where the z-dependent ZDW oscillates around the mean, similar to another proposed scheme⁸ showing improved CW FWM bandwidth. The composite fibre enables a FWM bandwidth of more than

70 nm, and allows for a time lens demonstration experiment accepting a WDM input signal spanning 13 nm with a flat -4.6-dB conversion efficiency over all WDM channels.

Composite fibre of optimally arranged segments of HNLF

Time lens systems based on FWM have a number of constraints, which are challenging to fulfil simultaneously. They rely on uniform phase-matching conditions for pump bandwidths demonstrated up to 1.6 THz⁶, good conversion efficiency to avoid signal-to-noise ratio degradations, and are sensitive to walk-off. Finally, the pump power is limited to below the onset of significant self-phase modulation. By using a DF-HNLF with low dispersion slope and a ZDW near the pump wavelength, the phase matching conditions can become uniform over a large pump bandwidth with low walk-off. However, hundreds of meters of fibre may be required to obtain sufficient conversion efficiency, and it is challenging to produce HNLFs with very low dispersion slope, while maintaining a stable ZDW for such lengths, and to reliably obtain a target average ZDW.

Fig. 1(a) shows the ZDW map for a ~1 km DF-HNLF, measured destructively with a resolution of 50 m. It can be seen that the ZDW varies by ~50 nm over the entire length, and by >15 nm for any contiguous 500-m segment. Although the impairment effects due to ZDW fluctuations are supposed to scale with the magnitude of the dispersion slope, such variations are expected to significantly impact

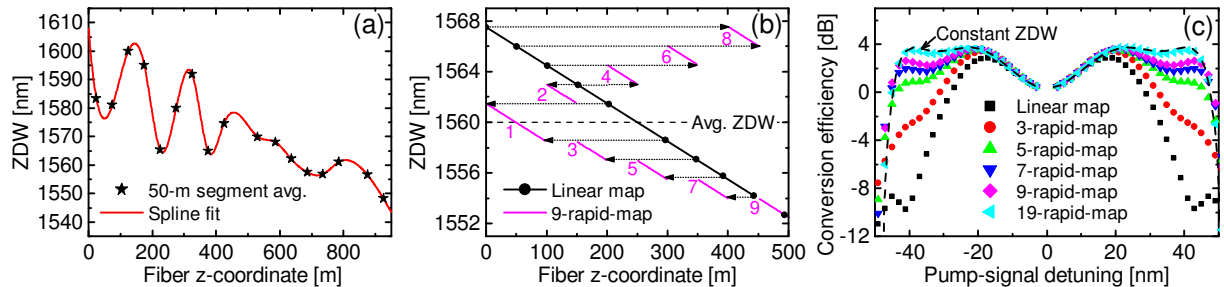


Fig. 1: Measured ZDW map over 950 m DF-HNLF (a), proposed rapid-map fibre rearrangement for the mitigation of ZDW fluctuation impairments in FWM (b) and pulsed conversion efficiency in DF-HNLF for various 15-nm variation ZDW maps (c)

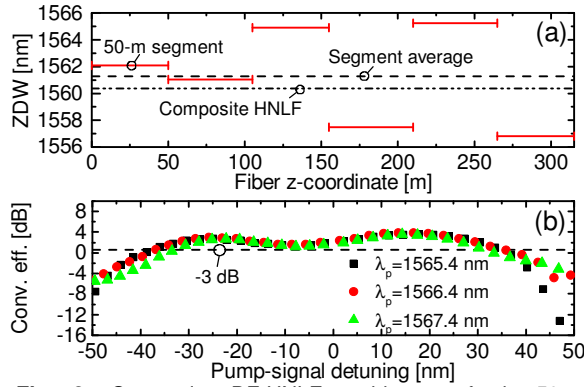


Fig. 2: Composite DF-HNLF rapid-map of six 50-m DF-HNLF segments (a) and CW conversion efficiencies (b)

the FWM bandwidth.

To reduce the impact of ZDW fluctuations on pulsed FWM, we propose to create a composite fibre of DF-HNLF segments to form a ZDW rapid-map. The segments are arranged so that the ZDW rapidly varies symmetrically around the mean ZDW. In this way the accumulated phase mismatch is imagined to become partially cancelled after each pair of opposite-dispersion segments. The effect of a rapid-map arrangement for a composite DF-HNLF fibre is investigated by solving the nonlinear Schrödinger equation with an adaptive split-step Fourier method including ZDW fluctuations. The change in ZDW is modelled as a vertical shift of the β_2 vs. frequency curve⁹. The simulated fibre has length 500 m, with average ZDW 1560 nm. The dispersion slope is 4.5×10^{-3} ps/(nm²·km), $\beta_4 = 2.6 \times 10^{-4}$ ps⁴/km and the nonlinear coefficient $\gamma = 10.8$ (W·km)⁻¹. The pulsed FWM conversion efficiency for four different rapid-maps and the original linear ZDW map is simulated. The rapid-maps are created from 3 segments (3-rapid-map) up to 19 segments (19-rapid-map). The 9-rapid-map is shown in Fig. 1(b), where the original fibre with linear variation is rearranged into 9 segments. In Fig. 1(c) the small-signal pulsed FWM conversion efficiency is shown for the different fibre arrangements. The pump is placed at 1565 nm with 25 dBm peak power, and pump and signal are 10-GHz, 50% duty cycle

Gaussian pulse trains. It can be seen that for faster variations with shorter segments the bandwidth improves, and using 25-m fibre segments efficiency close to that for constant ZDW is achieved.

To create a fibre for superior pulsed FWM performance, six of the ~50-m segments measured for Fig. 1(a) are combined into a 315-m composite DF-HNLF rapid-map. It is a useful feature that the average ZDW becomes a flexible design parameter with a sufficient number of segments. Here we choose a wavelength near 1560 nm to enable conversion between the C- and L-bands. The resulting ZDW map is shown in Fig. 2(a), indicating the average of the ZDWs measured for each segment (1561.3 nm), and the measured ZDW after splicing (1560.4 nm). The higher order dispersion and nonlinear coefficient are the same as for the simulated fibre. The losses are 0.02-0.04 dB for HNLF-to-HNLF splices, with an additional ~0.35 dB splice loss per end to attach intermediate-mode fibres and pigtails, for a total end-to-end loss of ~1 dB. The CW conversion efficiency was measured for pump wavelengths from 1565.4 nm to 1567.4 nm, with 28 dBm pump power launched into the fibre. Similar performances at the different pump wavelengths are achieved over 90 nm as shown in Fig. 2(b), indicating good phase matching uniformity, and more than 70 nm 3-dB bandwidth.

Experimental setup and pulsed FWM fibre characterisation

The performance of the composite DF-HNLF is tested in a time lens application⁵ with demanding pulsed FWM requirements. The conversion of 32 wavelength-division multiplexed (WDM) subcarriers spanning 13 nm is achieved using a broadband chirped pump, with a flat conversion efficiency of -4.6 dB. The setup is shown in Fig. 4. The WDM channels are generated from an array of distributed feedback lasers (DFBs) with 50-GHz spacing centred at 1546.3 nm, data modulated using a pseudo-random binary sequence (PRBS) with binary

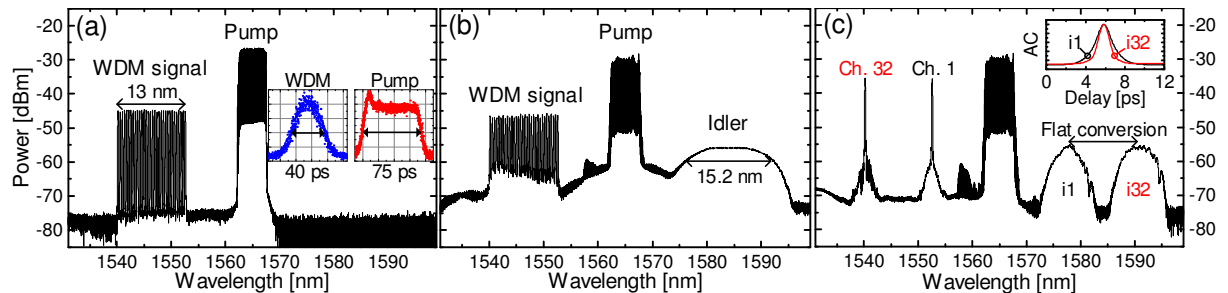


Fig. 3: FWM spectrum at the HNLF input with insets showing signal and pump waveforms (a), HNLF output spectrum with all WDM channels (b) and output spectrum with the outermost channels enabled and inset showing the ACs after the SSMF (c)

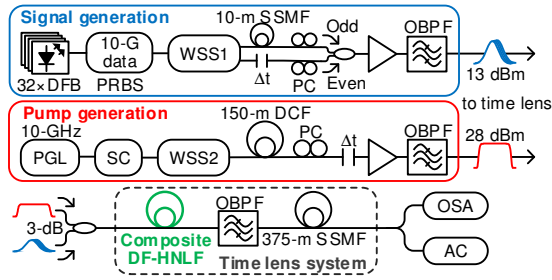


Fig. 4: Experimental setup for the fibre characterization. OBPF: Optical bandpass filter. Δt : Tunable time delay. PC: Polarization controller

phase-shift keying, and pulse carved with a 50% duty cycle at 10 GHz. The channels are decorrelated using a wavelength selective switch (WSS1) and amplified to 13 dBm using an erbium-doped fibre amplifier (EDFA). The pump is carved from a supercontinuum (SC) with WSS2 to obtain a rectangular spectrum, centred at 1565 nm with a bandwidth of 600 GHz. The SC is generated by SPM from propagation of ~ 1.5 -ps full-width at half maximum (FWHM) pulses at 1542 nm from a pulse-generating laser (PGL) in 400 m DF-HNLF. The pump spectrum is dispersed in 150 m dispersion-compensating fibre (DCF), obtaining a temporal FWHM of 75 ps, and chirp rate of $K/2 = 8$ GHz/ps. The pump is then amplified to 28 dBm average power in an EDFA. Finally, the pump and signal are aligned and coupled into the composite DF-HNLF using a 3-dB coupler. The HNLF input spectrum is shown in Fig. 3(a), with insets showing the WDM and pump waveforms. At the HNLF output the converted idler is filtered and dispersed in $L \sim 375$ m standard single-mode fibre (SSMF) to obtain accumulated dispersion $-\beta_2 L \sim 1/K$, in order to temporally focus the converted channels within different time slots. Finally, the spectrum is recorded using an optical spectrum analyser (OSA), and the autocorrelations (AC) for individually converted channels are measured. The composite DF-HNLF output spectrum for the conversion of all 32 channels can be seen in Fig. 3(b), showing a flat-top idler with ~ 15 -nm 3-dB bandwidth, indicating similar performance for all channels, and a -4.6-dB conversion efficiency. The conversion efficiency is obtained by comparing the integrated power of the idler spectrum with that of the input WDM spectrum. The spectrum with only the outermost WDM channels enabled is shown in Fig. 3(c), verifying a uniform conversion performance. The inset shows the AC after dispersion, revealing a small difference in temporal width. Assuming a Gaussian pulse shape, converted channel 1 (i1) has pulse width of 1.4 ps, whereas converted channel 32 (i32) has a pulse width of 1.1 ps,

with a target width after dispersion of ~ 1 ps. The discrepancy is thought to be due to differences in dispersion from propagation in the SSMF.

Conclusions

We demonstrate a composite dispersion-flattened HNLF for broadband pulsed FWM, consisting of segments positioned to reduce FWM impairments due to fluctuations of the zero-dispersion wavelength (ZDW). The conversion of a 13-nm WDM signal with a flat -4.6-dB FWM conversion efficiency is achieved in a demanding time lens demonstration experiment. Furthermore, numerical simulations indicate that this technique can close to completely compensate for linear ZDW fluctuations.

Acknowledgements

The authors would like to thank Lars Grüner-Nielsen, OFS, for illuminating discussions and for the fibres. This work was supported by the DFF Sapere Aude Adv. Grant, NANO-SPECs (DFF-4005-00558B).

References

- [1] M. Lillieholm et al., "Detailed Characterization of Continuous-Wave and Pulsed-Pump Four-Wave Mixing in Nonlinear Fibers," Proc. CLEO, SW4P.3, San Jose (2016).
- [2] S. Watanabe and M. Shirasaki, "Exact Compensation for both Chromatic Dispersion and Kerr Effect in a Transmission Fiber Using Optical Phase Conjugation", J. Lightw. Technol., Vol. **14**, no. 3, p. 243 (1996).
- [3] I. D. Phillips et al., "Exceeding the Nonlinear-Shannon Limit using Raman Laser Based Amplification and Optical Phase Conjugation", Proc. OFC, M3C.1, San Francisco (2014).
- [4] P. Guan et al., "All-Optical Ultra-High-Speed OFDM to Nyquist-WDM Conversion Based on Complete Optical Fourier Transformation," J. Lightw. Technol., Vol. **32**, no. 2, p. 626 (2016).
- [5] H. C. H. Mulvad et al., "DWDM-to-OTDM Conversion by Time-Domain Optical Fourier Transformation," Proc. ECOC, Mo.1.A.5, Geneva (2011).
- [6] H. Hu et al., "1.28 Tbaud Nyquist Signal Transmission using Time-Domain Optical Fourier Transformation based Receiver," Proc. CLEO, CTh5D.5, San Jose (2013).
- [7] B. P.-P. Kuo et al., "Dispersion-stabilized highly-nonlinear fiber for wideband parametric mixer synthesis," Opt. Express, Vol. **20**, no. 19, p. 18611 (2012).
- [8] K. Inoue, "Arrangement of fiber pieces for a wide wavelength conversion range by fiber four-wave mixing," Opt. Lett., Vol. **19**, no. 16, p. 1189 (1994).
- [9] L. S. Rishøj and K. Rottwitt, "Influence of Variations of the GVD on Wavelength Conversion at Second Gain Region of a Parametric Process," Proc. NP, NTuC11, Karlsruhe (2010).